Assessment of Postural Changes Before and After Hemodialysis Based on Body Weight Measurement Motion Using MediaPipe and Machine Learning

Yasutaka Uchida
Dept. of Life Science
Teikyo University of Science
Tokyo, Japan
e-mail: uchida@ntu.ac.jp

Kazuyoshi Hori
Dept. of Life Science
Teikyo University of Science
Tokyo, Japan
e-mail: hori-k@ntu.ac.jp

Ren Kondo
Dept. of Clinical Engineering
Katori Omigawa Medical Center
Chiba, Japan
e-mail: 0ys3272f7251v0s@ezweb.ne.jp

Satoshi Kidooka
Dept. of Clinical Engineering
Katori Omigawa Medical Center
Chiba, Japan
e-mail: kidooka@lilac.plala.or.jp

Sayuri Sugaya
Nursing Department
Katori Omigawa Medical Center
Chiba, Japan
e-mail: sugaya.sayuri@gmail.com

Tomoya Iizuka
Dept. of Clinical Engineering
Katori Omigawa Medical Center
Chiba, Japan
e-mail: pagupagu_tomoya@yahoo.co.jp

Abstract— **Post-dialysis unsteadiness in patients undergoing hemodialysis represents a significant clinical concern, as it increases the risk of falls and negatively affects prognosis and quality of life. However, conventional assessment methods used in clinical practice are often subjective, and simple, objective approaches for quantitatively evaluating post-dialysis unsteadiness remain insufficiently established. In this study, we propose a quantitative evaluation method for evaluating postural changes and unsteadiness by focusing on body weight measurement before and after hemodialysis and applying MediaPipe, a camera-based, non-contact pose estimation technique. Stepping onto a weighing scale requires balance control over a small base of support and can accentuate subtle alterations in postural stability. First, posture-related features were extracted through a preliminary study involving a small number of participants, and the structure of the extracted features was analyzed using principal component analysis, support vector machine, and k-means clustering. Subsequently, an expanded dataset was employed to evaluate the classification performance of pre- and post-dialysis conditions using machine learning. The results revealed discernible differences in postural stability before and after hemodialysis, indicating the effectiveness of the proposed approach. This study demonstrates the feasibility of a simple and objective method for assessing post-dialysis unsteadiness by combining camera-based pose estimation with machine-learning techniques, with potential applicability in clinical settings.**

Keywords-Hemodialysis; Post-dialysis unsteadiness; MediaPipe; Pose estimation; Machine learning; Support vector machine; k-means clustering.

I. INTRODUCTION

Unsteadiness and falls in patients undergoing hemodialysis constitute a significant clinical concern, profoundly impacting prognosis and quality of life (QOL). Following hemodialysis, rapid fluid shifts and reductions in blood pressure often lead to orthostatic hypotension and impaired postural control, thereby increasing the risk of falls. This risk is particularly pronounced among elderly hemodialysis patients, for whom falls can result in fractures, hospitalization, and a subsequent decline in long-term outcomes [1-5].

Given this background, the early and objective assessment of post-dialysis unsteadiness is crucial for ensuring patient safety and improving QOL. Conventional assessment methods commonly employed in clinical practice, however, often rely on subjective observations or simple balance tests, which may lack both objectivity and reproducibility. Although quantitative evaluations using force plates or wearable sensors, such as accelerometers, have been reported, their practical implementation is frequently constrained by installation complexity and operational demands [6-10].

In recent years, camera-based pose estimation techniques, which enable non-contact analysis of human posture, have garnered increasing attention in sports science and rehabilitation research. Methods such as OpenPose and MediaPipe Pose allow for the accurate extraction of body landmarks from video recordings and facilitate the calculation of indices such as postural sway and joint angle variability [11-14]. Our research group has previously demonstrated the clinical applicability of MediaPipe-based motion analysis through studies on gait assessment, evaluation of walking aid effects, investigation of error sources in pose estimation, and quantitative assessment analysis of gait changes in patients with hemiparesis [15].

Despite these advances, studies employing camera-based, non-contact pose estimation to quantitatively evaluate postural stability and unsteadiness in hemodialysis patients remain limited. In particular, few investigations have systematically examined feature extraction and machine-learning-based classification of pre- and post-dialysis conditions [1] [16].

Accordingly, this study focused on postural behavior during body weight measurement before and after hemodialysis and aimed to develop a method for quantitatively evaluating postural changes and unsteadiness using MediaPipe-based video analysis. As stepping onto a weighing scale requires maintaining balance over a small base of support and tends to accentuate subtle alterations in postural control, a preliminary study was conducted to identify effective features. Dimensionality reduction and clustering analyses were subsequently applied to explore the structure of the extracted features, followed by an assessment of pre- and post-dialysis classification performance using a support vector machine with an expanded dataset.

The remainder of this paper is organized as follows. Section II describes the participants, experimental setup, and measurement conditions. Section III presents the results of posture-related indices and joint angle calculations used for evaluation. Section IV provides a discussion of the findings, and Section V concludes the paper and outlines directions for future research.

II. EXPERIMENTS

A. Participants For Basic Feature Value Extraction

This preliminary experiment was conducted to identify effective feature values for the quantitative evaluation of post-dialysis unsteadiness. Four patients undergoing maintenance hemodialysis were recruited, and their demographic and clinical characteristics are summarized in Table I.

TABLE I. PARTICIPANT INFORMATION. PD AND UFR DENOTE PRIMARY DISEASE AND ULTRA-FILTRATION RATE

Subject	Age	Sex	Case of ESRD	ΔDW	ABI R	ABI L	Note
A	54	F	CG	4.2	1.10	1.17	BP reduced
B	62	M	Unknown	4.8	1.18	1.21	BP stable
C	78	M	DM	5.3	0.98	1.46	BP stable
D	51	M	DM	6.0	1.15	1.23	BP stable

Participants' selection was based on the presence of blood pressure fluctuations following dialysis and subjective symptoms of visual dizziness. This study was approved by the Ethics Committee of Katori Omigawa Medical Center, Katori, Japan (Approval No. 2024-3). Written informed consent was obtained from all participants prior to data collection.

B. Experimental Setup and Recording Conditions for Basic Feature Value Extraction

As illustrated in Figure 1, participants were recorded while standing still or shifting their posture on a body-weight scale. A consumer-grade video camera was positioned approximately 2 m in front of the participants to capture their movements. Owing to spatial constraints in the clinical environment, the camera was placed slightly above and to the left of each participant.

Figure 1. Experimental setup.

C. Data Acquisition and Skeletal Landmark Extraction for Basic Feature Value Extraction

Video data were processed using the Pose module of MediaPipe. The analysis was performed in a Jupyter Notebook using Python. MediaPipe extracted 3D skeletal landmarks (x, y, and z coordinates) for 33 body points. These coordinates, along with the visualization of the estimated skeletal structure overlaid on the video frames, were saved in comma-separated value (CSV) format for subsequent analysis.

D. Postural Indices and Joint-Angle Computation for Basic Feature Value Extraction

To evaluate postural changes before and after hemodialysis, a set of approximated joint angles (hereafter referred to as "approximated angles") was defined, as illustrated in Figure 2. The following six metrics were used:

(1) Approximated trunk forward tilt angle (TFTA): Defined as the angle formed between the trunk axis (midpoints of the shoulders and hips) and the lower-limb axis (midpoints of the hips and knees).

(2) Approximated cervical flexion angle (CFA): Defined as the angle between the line connecting both shoulders to the nose and the line connecting the midpoint of both hips to the midpoint of the shoulders.

(3) Approximated shoulder abduction angle (SAA_L of SAA_R): Calculated using the positions of the shoulder and elbow joints for the left and right sides, respectively.

(4) Approximated elbow flexion angle (EFA): Calculated as the angle formed by the wrist, elbow, and shoulder joints.

(5) Approximated knee flexion angle (KFA): Calculated as the joint angle formed by the hip, knee, and ankle joints.

(6) Approximated hip flexion angle (HFA): Defined as the angle between the extended trunk axis and the lower-limb axis.

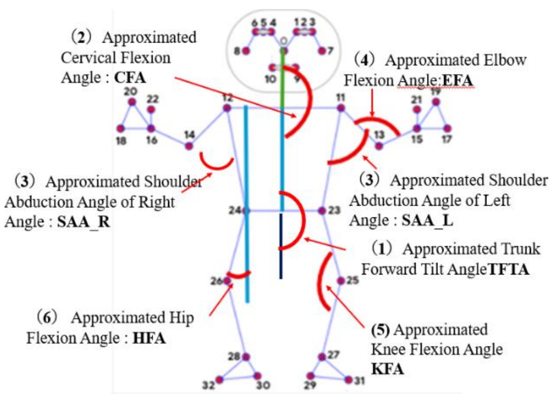

Figure 2. Definitions of the approximated joint angles.

Each angle was calculated using the following formula, based on the inner product of two vectors $\vec{A}$ and $\vec{B}$.

$$\theta = \cos^{-1}\left(\frac{\vec{A}\cdot\vec{B}}{\|\vec{A}\|\cdot\|\vec{B}\|}\right) \quad (1)$$

The vectors were derived from the coordinate data stored in the CSV files. Given that the video recordings were obtained from a slightly left upper oblique angle relative to the participants, all computed values were interpreted as approximated angles rather than exact anatomical measurements.

.

III. Experimental Results

A. Preliminary Feature Extraction Using Four Participants

1) Qualification of nasal sway for basic feature extraction: Figure 3 illustrates an example of nasal-position fluctuations for participant A while standing on a weighing scale. Figures 3(1) and 3(2) correspond to the pre-dialysis and post-hemodialysis conditions, respectively. The recording time before hemodialysis was shorter because of the simultaneous measurement of body weight. Although identical measurement durations would be preferable, no special instructions were provided to the participants, who followed their usual clinical procedures.

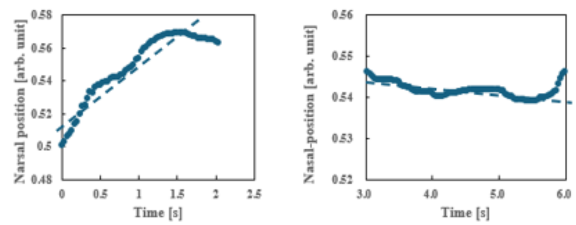

(1) (2)

Figure 3. Example of nasal position displacement during body weight measurement in the preliminary experiment: (1) pre-dialysis and (2) post-hemodialysis conditions.

To eliminate the consistent directional drift, a linear correction was applied to the x-axis nasal-position data, adjusting the overall mean to zero. The corrected data are presented in Figure 4. The degree of nasal sway was calculated as the difference between the maximum positive and negative peaks, with red circles indicating the corresponding time points. Additionally, if the values reached the measurement-range boundaries without forming distinct peaks, they were counted as peak points. The number of transitions in the right and left directions is summarized in Table II.

Prior to hemodialysis, all participants exhibited a consistent difference in the number of directional transitions between rightward and leftward movements. Therefore, this index may serve as a useful quantitative indicator of postural changes associated with hemodialysis.

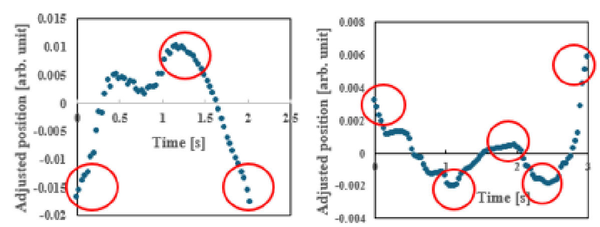

(1) (2)

Figure 4. Linearly corrected nasal position data used for quantification of nasal sway in the preliminary feature extraction experiment: (1) pre-dialysis and (2) post-hemodialysis conditions.

TABLE II. Number of Right-Left directional Transitions of Nasal Sway in the Preliminary feature Extraction Experiment

		Before	R-L	After	R-L
A	L	1	1	3	-1
	R	2		2	
B	L	1	1	2	0
	R	2		2	
C	L	2	1	3	0
	R	3		3	
D	L	1	1	2	1
	R	2		1	

Figure 5 presents the time-series differential analysis of the x-axis nasal position, performed to detect subtle postural fluctuations that are not readily apparent in the raw displacement data. Changes in the sign of the differential were used to identify reversals in the direction of nasal movement, thereby enabling quantification of directional transitions as an index of postural control.

These results indicate that nasal sway characteristics derived from differential analysis may serve as effective features for evaluating postural changes associated with hemodialysis.

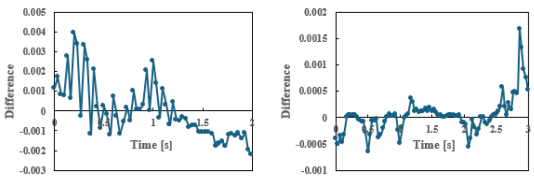

(1) (2)

Figure 5. Time-series differential analysis of the x-axis nasal position used to identify directional reversals and quantify nasal sway transitions: (1) pre-dialysis and (2) post-hemodialysis conditions.

2) Approximated trunk forward tilt angle (TFTA): As a representative example, the results for Subject B, who exhibited a pronounced change in trunk posture, are presented. The mean trunk forward tilt angle for Subject B was 163° before hemodialysis, decreasing to 136° after hemodialysis, indicating an increase in forward trunk inclination.

Although the median is generally considered more robust to outliers than the mean, the difference between the mean and median values in this study fell within the range of measurement error. Accordingly, the mean value was adopted as the representative index for evaluating trunk forward tilt.

3) Approximated cervical flexion angle (CFA): Figure 6 illustrates representative changes in the approximated cervical flexion angle (CFA) for Subject B. Figures 6(1) and 6(2) correspond to the pre-dialysis and post-dialysis conditions, respectively. The mean CFA decreased from 163° before hemodialysis to 146° after hemodialysis, indicating an increase in forward head posture and cervical flexion. These changes suggest possible alterations in postural control following hemodialysis.

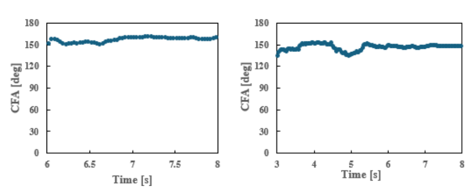

(1) (2)

Figure 6. Approximated cervical flexion angle (CFA) for Subject B: (1) pre-dialysis and (2) post-dialysis conditions.

4) Approximated shoulder abduction angle of left and right (SAA_L and SAA_R): Figure 7 presents representative results for the left shoulder abduction angle (SAA_L) of Subject A, with Figures 7(1) and 7(2) corresponding to the pre-dialysis and post-dialysis conditions, respectively. A pronounced change in SAA_L was observed for this subject, with the mean angle decreasing from 14° before hemodialysis to approximately 8° after hemodialysis, representing a reduction of nearly 50%.

In contrast, the right shoulder abduction angle (SAA_R) for the same subject changed by less than 1°. Although not shown in the figure, Subject D exhibited the opposite trend, with a pronounced change in SAA_R, decreasing from approximately 30° to 15° after hemodialysis. These asymmetric changes may reflect individual differences in posture and arm dominance, as well as the influence of an oblique camera angle during data acquisition.

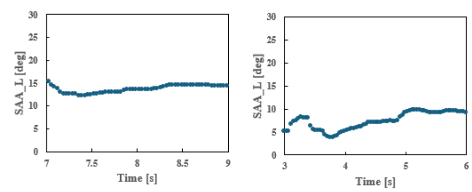

(1) (2)

Figure 7. Approximated left shoulder abduction angle (SAA_L) for Subject A: (1) pre-dialysis and (2) post-dialysis conditions.

5) Approximated elbow flexion angle (EFA): Figure 8 illustrates representative changes in the left elbow flexion angle (EFA) for Subject C, with Figures 8(1) and 8(2) corresponding to the pre- and post-dialysis conditions, respectively. The angel increased from 105° before hemodialysis to 112° after hemodialysis, indicating enhanced elbow flexion following treatment.

Although the absolute angle values differed from those observed in Subjects A and D, a similar trend of increased flexion after hemodialysis was noted. In contrast, Subject B exhibited a slight decrease in elbow flexion. These findings indicate that elbow flexion may reflect individual postural adaptations to hemodialysis, although inter-subject variability should be taken into account.

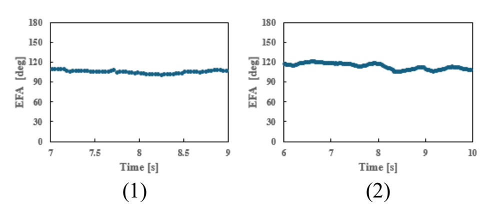

(1) (2)

Figure 8. Approximated left elbow flexion angle (EFA) for Subject C: (1) pre-dialysis and (2) post-dialysis conditions.

6) Approximated knee flexion angle (KFA): Figure 9 presents the knee flexion angle for Subject D under preand post-dialysis conditions. The angle increased from 167° prior to hemodialysis to 180° following hemodialysis, indicating a transition toward near-complete knee extension.

Similar tendencies toward increased knee extension were observed in other participants; however, the magnitude of these changes was relatively small compared with those observed for upper-body postural indices. These findings suggest that, within the present measurement framework, detecting subtle post-dialysis changes based solely on knee flexion alone may be challenging.

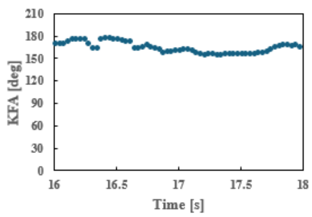

(1)

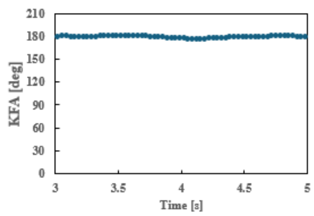

(2)

Figure 9. Approximated knee flexion angle (KFA) for Subject D: (1) pre-dialysis and (2) post-dialysis conditions.

7) Approximated hip flexion angle (HFA): Although the hip flexion angle is conventionally evaluated during gait, this study assessed the parameter under static standing conditions. Owing to the short recording duration and the oblique positioning of the camera, measurement accuracy was inherently limited.

Despite these constraints, directional changes in hip flexion angle were observed in two participants, suggesting that this parameter may partially reflect physiological or postural alterations associated with hemodialysis. Improvements in measurement precision, as well as the incorporation of dynamic motion analysis, may enable a more comprehensive and reliable evaluation in future studies.

A summary of all calculated postural indices is presented in Table III.

TABLE III. SUMMARY OF MEASURED VALUES FOR EACH POSTURAL EVALUATION INDEX

		nose	TFTA	CFA	SAA_Left	SAA_Right	EFA	KFA
		Dif	deg	deg	deg	deg	deg	deg
A	BFR	6.50E-02	161	147	14.3	19.3	100	166
	AFT	7.70E-03	177	137	7.70	13.1	118	140
	Ratio	0.11	1.10	0.93	0.54	0.68	1.18	0.84
B	BFR	7.20E-02	163	163	18.0	9.60	120	160
	AFT	5.60E-02	136	146	13.3	14.7	112	161
	Ratio	0.78	0.83	0.90	0.74	1.53	0.93	1.00
C	BFR	2.60E-02	165	156	20.3	30.3	105	149
	AFT	3.20E-02	165	152	23.5	26.8	112	149
	Ratio	1.23	1.00	0.97	1.16	0.88	1.07	1.00
D	BFR	4.30E-02	152	151	24.8	30.6	116	167
	AFT	4.10E-02	154	142	22.1	14.7	124	180
	Ratio	0.95	1.01	0.94	0.89	0.48	1.07	1.08

8) Spectral analysis of knee movement: To further assess postural stability, a time–frequency analysis was performed on the lateral (x-axis) knee position data obtained using MediaPipe. Although the recording duration was brief, a discrete Fourier transform (DFT) with a 1 s sliding window was applied to generate spectrograms representing temporal variations in frequency components [17-19].

The input signals were derived from 30-fps video data, resulting in a Nyquist frequency of 15 Hz. The spectrograms were visualized with time on the horizontal axis and frequency on the vertical axis. Spectral magnitude (the square root of the power spectrum) at each time–frequency coordinate was represented using a five-level color gradient, ranging from black (minimum) to red (maximum).

Figure 10 presents a representative example for Subject A, with panels (1) and (2) corresponding to the left and right knees, respectively. The observed spectral patterns reveal subtle temporal fluctuations in knee motion that are not readily detectable using angle-based analyses alone.

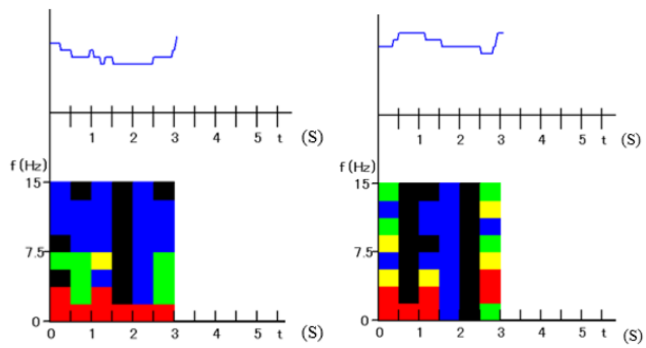

(1) (2)

Figure 10. Time–frequency spectrogram of lateral knee movement for Subject A: (1) left knee and (2) right knee.

B. Feature Analysis and Machine-Learning-Based Exploration Using the Expanded Dataset

1) Feature selection based on preliminary analysis: Based on the results of the preliminary feature extraction study, the participant cohort was expanded by adding 18 subjects, yielding a total of 22 participants for subsequent analyses. In the present measurements, no prior instructions were provided to the participants in order to capture images during routine body weight measurement in a clinical setting. Consequently, substantial inter-subject variability was observed in both the duration of standing on the weighing scale and the movement of the upper limbs.

To ensure consistency across participants, the analysis in the latter phase was restricted to a 2 s image segment for each subject. Consequently, the observation period for nasal position fluctuations was considerably shorter than that employed in the preliminary feature extraction study, making it difficult to detect differences between pre- and post-dialysis conditions. For this reason, nasal sway–related features were excluded from the analyses conducted using the expanded dataset.

2) Visualization of feature distributions and class separability: To examine the characteristics of the selected feature sets and their discriminative potential between pre- and post-dialysis conditions, exploratory visualizations were performed using the expanded dataset consisting of 22 participants. As described in Section B-1, the analysis was restricted to a 2 s image segment for each participant, and nasal sway-related features were excluded.

Figure 11 (at the end of the paper) illustrates the distributions of representative features for the pre- and post-dialysis classes, visualized using seaborn. These plots facilitate qualitative comparisons of central tendency and variability between classes and enable the identification of features exhibiting noticeable shifts following hemodialysis. Although several features exhibit substantial overlap between the two distributions, others demonstrate class-dependent trends, suggesting potential relevance for discriminative analysis [20][21].

Figure 12 (at the end of paper) presents pairwise relationships among the selected features, visualized using scatter plots with class labels. These plots provide insight into the degree of class separation in low-dimensional feature spaces and reveal correlations among features. In several projections, partial separation between pre- and post-dialysis samples is apparent, whereas other combinations exhibit substantial overlap, indicating redundancy or limited discriminative power.

Overall, the seaborn-based visualizations highlight differences in distributional characteristics and inter-feature relationships across feature sets. These qualitative observations guided the selection of feature sets for subsequent machine-learning-based classification, as described in the following section.

To ensure consistency across participants, the analysis in the latter phase was restricted to a 2 s image segment for each subject. Consequently, the observation period for nasal position fluctuations was considerably shorter than that employed in the preliminary feature extraction study, making it difficult to detect differences between pre- and post-dialysis conditions. For this reason, nasal sway–related features were excluded from the analyses conducted using the expanded dataset.

3) Principal component analysis: Although six candidate features were selected through initial screening, principal component analysis (PCA) was performed to determine which components efficiently capture the underlying data structure and contribute to class separability. PCA was applied to project the high-dimensional feature space onto a lower-dimensional space, facilitating visualization of inter-feature relationships and distributional characteristics [22] [23].

Because predefined class labels were not available for the analyzed dataset, a data-driven pseudo-labeling strategy based on PCA was employed. Specifically, the two-dimensional PCA space defined by the first and second principal components (PC1–PC2 plane) was partitioned into four quadrants according to the signs of the principal component scores:

Q1: $\mathrm{PC1} \geq 0$ and $\mathrm{PC2} \geq 0$

Q2: $\mathrm{PC1} < 0$ and $\mathrm{PC2} \geq 0$

Q3: $\mathrm{PC1} < 0$ and $\mathrm{PC2} < 0$

Q4: $\mathrm{PC1} \geq 0$ and $\mathrm{PC2} < 0$

Each sample was assigned to one of the four quadrants (Q1–Q4), and the resulting quadrant labels were used as pseudo labels for subsequent supervised learning. This labeling approach relies exclusively on the geometric structure of the PCA space and does not require manual annotation or predefined threshold values.

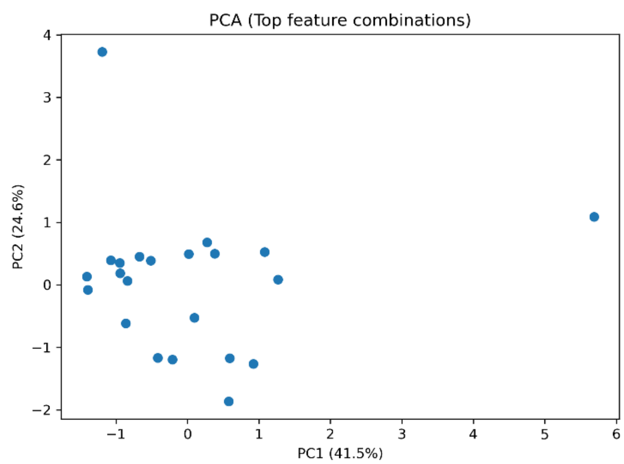

Figure 13. Example of the data distribution in the PCA space obtained using the selected feature set.

The PCA plane was divided into four quadrants based on the signs of the principal component scores, and each sample was assigned to one of the quadrants (Q1–Q4) for data-driven pseudo-labeling.

PC2 represents an asymmetry-related component rather than a global magnitude of motion. This component is primarily influenced by features associated with left–right differences in shoulder abduction, as indicated by loadings with opposite signs for N_SAA_L and N_SAA_R. Notably, the interpretation of PC2 does not depend on the sign of the axis itself; rather, the magnitude along PC2 reflects the degree of asymmetry in upper-body posture and coordination.

4) Support vector machine analysis: Based on the PCA results, it was suggested that classification could be feasible using two principal components. Consequently, support vector machine (SVM) classification was performed using these components as input features, employing two types of kernels: a linear kernel and a Gaussian radial basis function (RBF) kernel [24].

The classification results obtained using the linear kernel are shown in Figure 14, while those obtained using the Gaussian RBF kernel are presented in Figure 15. The first principal component (PC1) is considered to represent the overall magnitude of body movement and postural variation between pre- and post-dialysis conditions, whereas the second principal component (PC2) reflects asymmetry-related postural characteristics.

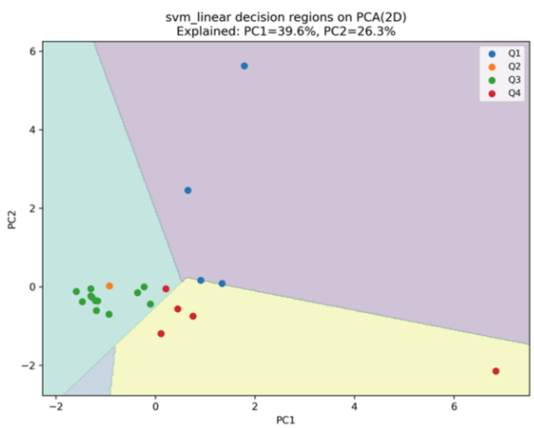

Figure 14. Linear SVM classification in the PC1–PC2 space.

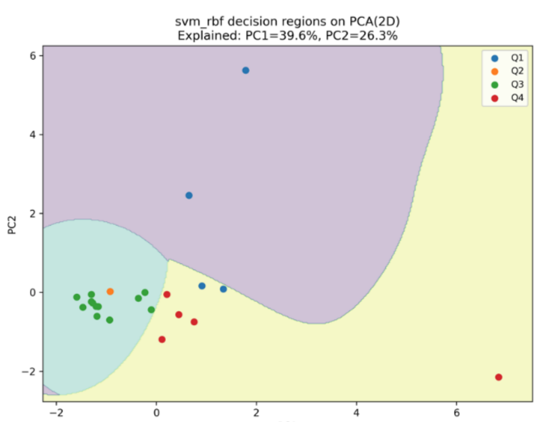

Figure 15. RBF-kernel SVM classification in the PC1–PC2 space.

5) K-means Clustering Analys: To further explore the inherent structure of the feature space without reliance on predefined labels, K-means clustering was applied. The optimal number of clusters was determined using the elbow method, in which the within-cluster sum of squares (inertia) was evaluated as a function of the number of clusters k [25].

Figure 16 illustrates the relationship between k and inertia. A pronounced decrease in inertia is observed up to $k = 3$, followed by a more gradual decline for larger values of k, indicating an elbow point at $k = 3$. Accordingly, the number of clusters was set to three for subsequent analyses.

Figure 17 presents the clustering results obtained with $k = 3$. The samples are partitioned into three groups within the feature space, reflecting distinct patterns in postural characteristics. These clusters provide an unsupervised perspective on the underlying data structure and offer complementary insight to the PCA-based and SVM-based analyses.

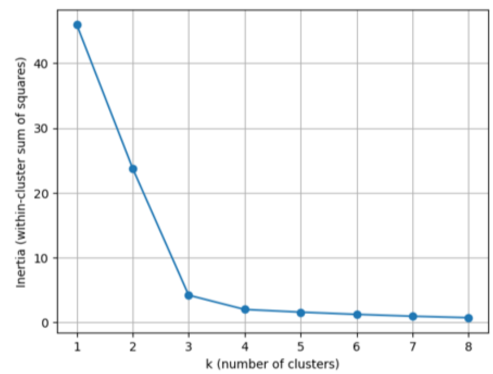

Figure 16. Elbow method for K-mean*s* clustering showing the relationship between the number of clusters (k) and inertia (within-cluster sum of squares), with an elbow point observed at $k = 3$.

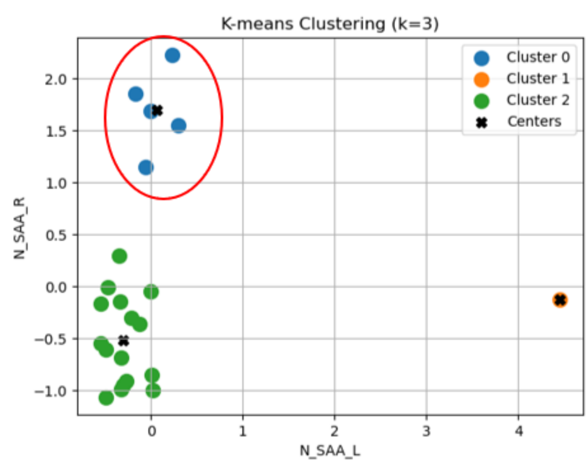

Figure 17. Results of K-mean*s* clustering with $k = 3$, illustrating the partitioning of samples into three clusters in the feature space.

IV. Discussion

A. Nasal Displacement (Sway)

No specific instructions were provided to either the staff or participants regarding the measurement process.

Consequently, variability was observed in the timing of body-weight measurements and the duration of video recording. This variability should be considered when interpreting the results, and standardization of measurement conditions is recommended for future studies.

As shown in Table I, four participants exhibited the same number of lateral movements along the x-axis of the nose before hemodialysis. This finding suggests that pre-dialysis movements followed a consistent pattern, and that differences in movement count could serve as a quantitative indicator of postural sway or instability.

Without applying a linear correction to the nasal x-axis data, the observed movement tended to form a plateau, biased in a constant direction, which made it difficult to define motion boundaries. Nevertheless, measuring the duration of such sustained bias may provide an alternative evaluation metric.

Moreover, time-series differencing of nasal-position data can capture subtle movements. Applying a DFT to these differential data may enable the extraction of periodicity or distinctive frequency components, highlighting the potential for advanced sway analysis and quantitative assessment of individual differences.

B. *Estimated Cervical Flexion Angle*

Figure 6 illustrates the changes in estimated cervical flexion angles. For Participant B, the mean angle decreased from 163° before hemodialysis to 146° after hemodialysis, indicating an increase in cervical flexion. This change may reflect forward head posture or alterations in neck alignment following hemodialysis, potentially associated with physical fatigue or altered postural control.

C. *Estimated Elbow Flexion Angle*

An increase in elbow flexion angle may indicate changes in muscle tone or enhanced body stability. In contrast to Participant B, these results underscore the significance of individual variations. Additionally, differences between the dominant and nondominant limbs—including the presence of a hemodialysis shunt—should be considered in future investigations.

D. *Estimated Knee Flexion Angle*

A trend toward full extension (approaching 180°) was observed, which may reflect muscle relaxation or changes in standing posture stability. However, measurement errors resulting from oblique camera angles, rather than frontal views, may have also contributed to this outcome.

E. *Estimated Hip Flexion Angle*

Although hip flexion is typically evaluated during gait, this study employed a brief static assessment with participants standing on a scale and the camera positioned obliquely. These conditions limit the precision of angle estimation. Nevertheless, the observed differences in flexion direction between participants suggest postural or physiological changes induced by hemodialysis. High-precision measurements and evaluations during motion are expected to enable more detailed analysis in future studies.

Table IV (at the end of the paper) summarizes the evaluations at each estimated joint-angle point based on the results and discussion. Changes of 5% or more but less than 10% are indicated by the symbol ○, while changes of 10% or more are indicated by the symbol ◎. Given the variability in each participant's health status, correlations incorporating individual health conditions will also be necessary.

The intradialytic weight loss (%) was 4.2%, 4.8%, 5.3%, and 6.0% for Subjects A, B, C, and D, respectively. Although the present results focused on postural changes and did not directly reflect these fluid removal rates, a more accurate evaluation could be achieved by conducting a comprehensive analysis that integrates the indicators examined in this study with individual physical function data and relevant clinical information, such as medication.

F. *Spectrogram*

Because the spectral intensity is obtained as a function of time, variations in the frequency components can be analyzed and used to improve the accuracy of motion assessment by correlating them with the corresponding video frames. In the present measurements, however, the upper frequency limit was set to 15 Hz with a temporal resolution of 0.5 s.

G. *PCA-based Analysis and Pseudo Labeling*

PCA revealed that the selected postural features form a structured distribution in a low-dimensional space, despite substantial inter-subject variability and the absence of predefined class labels. This finding suggests that the extracted features capture meaningful postural characteristics associated with hemodialysis-related changes.

By projecting the data onto the first two principal components and partitioning the PCA space into four quadrants, a data-driven pseudo-labeling strategy was established without relying on manual annotation or predefined thresholds. This approach enabled objective grouping of samples based solely on the geometric structure of the feature space. In contrast to conventional labeling schemes that depend on clinical criteria or subjective judgments, the proposed method provides a reproducible and unbiased alternative for downstream supervised learning.

The observed separation patterns in the PCA space indicate that postural changes associated with hemodialysis are not sufficiently characterized by a single scalar feature, but instead emerge from combinations of multiple postural indices. Notably, upper-body-related features, such as trunk inclination and cervical flexion, contributed more strongly to variance along the principal components than lower-limb features, which demonstrated limited sensitivity under the present measurement conditions.

It should be noted, however, that the PCA-based quadrant labeling does not imply a direct correspondence to clinical states or symptom severity. Rather, it provides a coarse but effective partitioning of the feature space that facilitates supervised classification in subsequent analyses. Future studies incorporating larger datasets and clinically validated outcome measures may enable refinement of the labeling strategy and improve interpretability with respect to physiological or functional states.

Overall, the PCA-based analysis demonstrates that the combination of unsupervised dimensionality reduction and data-driven labeling constitutes a feasible approach for analyzing posture-related data acquired under unconstrained clinical conditions. This framework is particularly well-suited to exploratory studies in which explicit class definitions are unavailable or difficult to establish.

H. SVM Analysis

The observed difference in performance between linear and RBF SVMs suggests that the structure of the PCA space is partially non-linear, particularly among subjects with heterogeneous clinical backgrounds.

I. K-means Analysis

The subjects in the group highlighted in red were relatively younger than the others. Based on this difference, it is necessary to analyze individual characteristics, including dialysis conditions and medical history, to better understand the factors influencing postural clustering patterns.

V. Conclusion

This study investigated postural changes before and after hemodialysis using camera-based, non-contact pose estimation in combination with machine-learning techniques. A preliminary analysis involving four participants was conducted to identify candidate postural features, followed by validation using an expanded dataset comprising 22 participants.

The results demonstrated that upper-body–related features, including trunk inclination, cervical flexion, and shoulder posture, captured meaningful changes associated with hemodialysis, whereas lower-limb features exhibited limited sensitivity under the present measurement conditions. Principal component analysis revealed a structured distribution within a low-dimensional feature space, enabling data-driven pseudo-labeling without predefined class definitions. Using these labels, support vector machine classification and K-mean*s* clustering further confirm the presence of consistent postural patterns.

Overall, the findings indicate that the integration of non-contact pose estimation with unsupervised and supervised learning provides a feasible and objective framework for evaluating post-dialysis postural changes under unconstrained clinical conditions. This approach has the potential to support simple and quantitative assessment of postural instability in hemodialysis patients. Future work will focus on expanding the dataset, enhancing measurement robustness, and establishing clinical relevance through comparison with conventional balance assessments.

Acknowledgment

We are grateful to the patients and medical staff of Katori Omigawa Medical Center for their cooperation with this study. We also thank Associate Prof. T. Funayama and Emeritus Prof. Y. Kogure for helpful discussions. This study was partly supported by a JSPS Grant-in-Aid for Scientific Research (Issue no. JP23K11207).

References

[1] Y. Uchida et al., "Postural-Change Detection Before and After Hemodialysis Using MediaPipe," GLOBAL HEALTH 2025, IARIA, pp. 1–6, 2025.

[2] R. G. Roberts, R. A. Kenny, and E. J. Brierley, "Are elderly haemodialysis patients at risk of falls and postural hypotension?", International Urology and Nephrology, vol. 35, pp. 415–421, 2003.

[3] A. Mol, P. T. S. Bui Hoang, S. Sharmin, R. J. A. van Wezel, C. G. M. Meskers, and A. B. Maier, "Orthostatic Hypotension and Falls in Older Adults: A Systematic Review and Meta-analysis," Journal of the American Medical Directors Association, vol. 20, no. 5, pp. 589–597.e5, 2019.

[4] M. Kanbay et al., "An update review of intradialytic hypotension: concept, risk factors, clinical implications and management," Clinical Kidney Journal, vol. 13, no. 6, pp. 981–993, 2020.

[5] S. M. Hamrahian, S. Vilayet, J. Herberth, and T. Fülöp, "Prevention of Intradialytic Hypotension in Hemodialysis Patients: Current Challenges and Future Prospects," International Journal of Nephrology and Renovascular Disease, vol. 2023, pp. 173–181, 2023.

[6] L. A. da S. de Jesus et al., "Factors associated with postural balance in patients with end-stage renal disease on hemodialysis," Clinical Biomechanics, vol. 107, 106033, 2023.

[7] N. Shirai et al., "Dysfunction in dynamic, but not static balance is associated with risk of accidental falls in hemodialysis patients: a prospective cohort study," BMC Nephrology, vol. 23, Art. no. 237, 2022.

[8] H. Zhou et al., "Hemodialysis Impact on Motor Function beyond Aging and Diabetes—Objectively Assessing Gait and Balance by Wearable Technology," Sensors, vol. 18, no. 11, 3939, 2018.

[9] L. M. F. Lucinda et al., "SP420 Postural Balance in Patients Undergoing Hemodialysis," Nephrology Dialysis Transplantation, vol. 34, Suppl. 1, gfz103.SP420, 2019.

[10] A. Capitanini et al., "Multidimensional Assessment of Physical Function for People in Dialysis: The REACT Study," Kidney and Blood Pressure Research, vol. 49, no. 1, pp. 1026–1032, 2024.

[11] A. Komeili, B. Rajaei, "OpenPose vs MediaPipe: How Two Leading Frameworks Are Transforming Pose Estimation in

2025," saiwa.ai, https://saiwa.ai/blog/openpose-vs-mediapipe/ 2026.3.5

[12] K. Morker, "MediaPipe vs. OpenPose: A Practical Guide to Pose Analysis," DhiWise, https://www.dhiwise.com/post/mediapipe-vs-openpose-a-practical-guide-to-pose-analysis/ 2026.3.5

[13] C. S. T. Hii, K. B. Gan, N. Zainal, N. M. Ibrahim, and S. Azmin, "Frontal Plane Gait Assessment Using MediaPipe Pose," Proceedings of the 8th International Conference on Space Science and Communication, Springer Proceedings in Physics, vol. 303, pp. 347–356, 2024, , doi: 10.1088/1757-899X/1279/1/012004.

[14] Y. Uchida, T. Funayama, E. Ohkubo, D. Souma, and Y. Kogure, "Detecting Gait Changes with Front-Facing Video and MediaPipe: A Hemiplegic Patient Case Study," GLOBAL HEALTH 2024, IARIA, pp. 1–6, 2024.

[15] Y. Uchida, T. Funayama, E. Ohkubo, D. Souma, and Y. Kogure, "Detection of Changes in Lateral Weight Shift During Gait Improvement of Patients via Image Analysis of Frontal-Direction Imaging Using MediaPipe", International J. of Advances in Life science, vol.17, pp.19-30 no. 1 & 2, 2025.

[16] F. Roggio, B. Trovato, M. Sortino, and G. Musumeci, "A comprehensive analysis of machine learning pose estimation models used in human movement and posture analyses: A narrative review," Heliyon, vol. 10, no. 21, e39977, 2024.

[17] C. Francia et al., "Validation of a MediaPipe System for Markerless Motion Analysis During Virtual Reality Rehabilitation," Lecture Notes in Computer Science, vol. 15029, pp. 40–49, 2024.

[18] A. Gupta, P. L. Shrestha, B. Thapa, R. Silwal, and R. Shrestha, "Knee Flexion/Extension Angle Measurement for Gait Analysis Using Machine Learning Solution 'MediaPipe Pose' and Its Comparison with Kinovea®," IOP Conference Series: Materials Science and Engineering, vol. 1279, 012004, 2023.

[19] Y. Aoyama and H. Tanaka, "Automatic Analysis of Gait Cycle Using MediaPipe," ISASE 2023, pp. 1–13, 2023.

[20] M. Waskom, "seaborn: statistical data visualization," seaborn 0.13.2 Documentation, 2024. Available from: https://seaborn.pydata.org/ 2026.3.5

[21] S. Yıldırım, "Analyzing Data Distributions with Seaborn," Towards Data Science, 2020. Available from: https://towardsdatascience.com/analyzing-data-distributions-with-seaborn-a8607961a212/ 2026.3.5.

[22] G. Ivosev, L. Burton, and R. Bonner, "Dimensionality Reduction and Visualization in Principal Component Analysis," Analytical Chemistry, vol. 80, pp. 4933–4944, 2008.

[23] N. Migenda, R. Möller, and W. Schenck, "Adaptive dimensionality reduction for neural network-based online principal component analysis," PLOS ONE, vol. 16, no. 3, e0248896, 2021.

[24] A. Mehta, P. Sengupta, D. Garg, H. Singh, and Y. S. Diamand, " Benchmarking the Effectiveness of Classification Algorithms and SVM Kernels for Dry Beans," arXiv:2307.07863, 2023.

[25] I. Herdiana, M. A. Kamal, Triyani, M. N. Estri, and Renny, "A More Precise Elbow Method for Optimum K-means Clustering," arXiv:2502.00851, 2025.

TABLE IV. EVALUATION RESULTS

		nose	TFTA	CFA	SAA_Left	SAA_Right	EFA	KFA
		Dif	deg	deg	deg	deg	deg	deg
A	Ratio	◎	◎	○	◎	◎	◎	◎
B	≧5% ○	◎	◎	○	◎	◎	X	X
C	≧10%	◎	X	X	◎	◎	X	X
D	◎	○	X	○	◎	◎	X	○

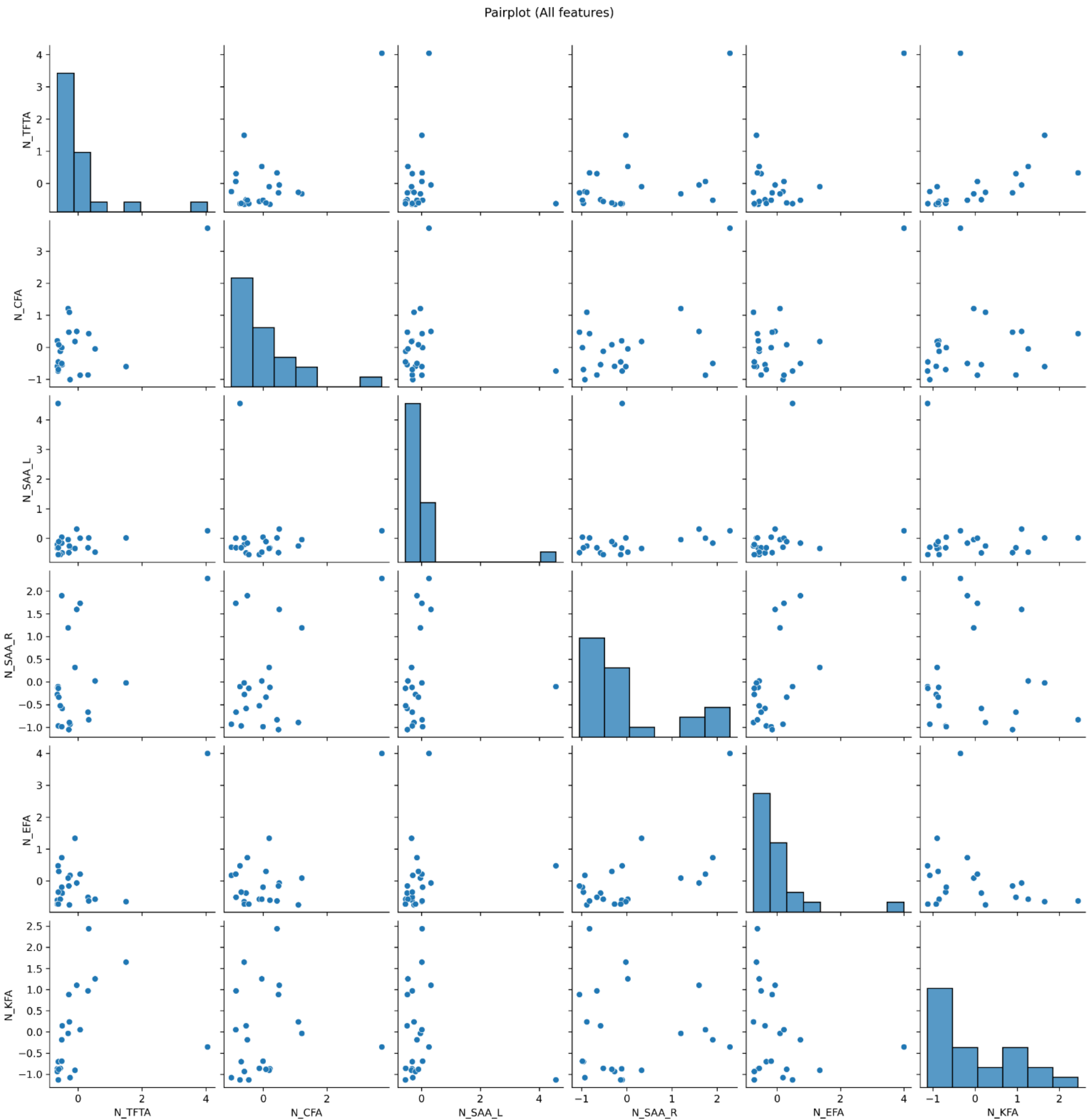

Figure 11. Exploratory visualization of six candidate feature sets derived from the preliminary study.

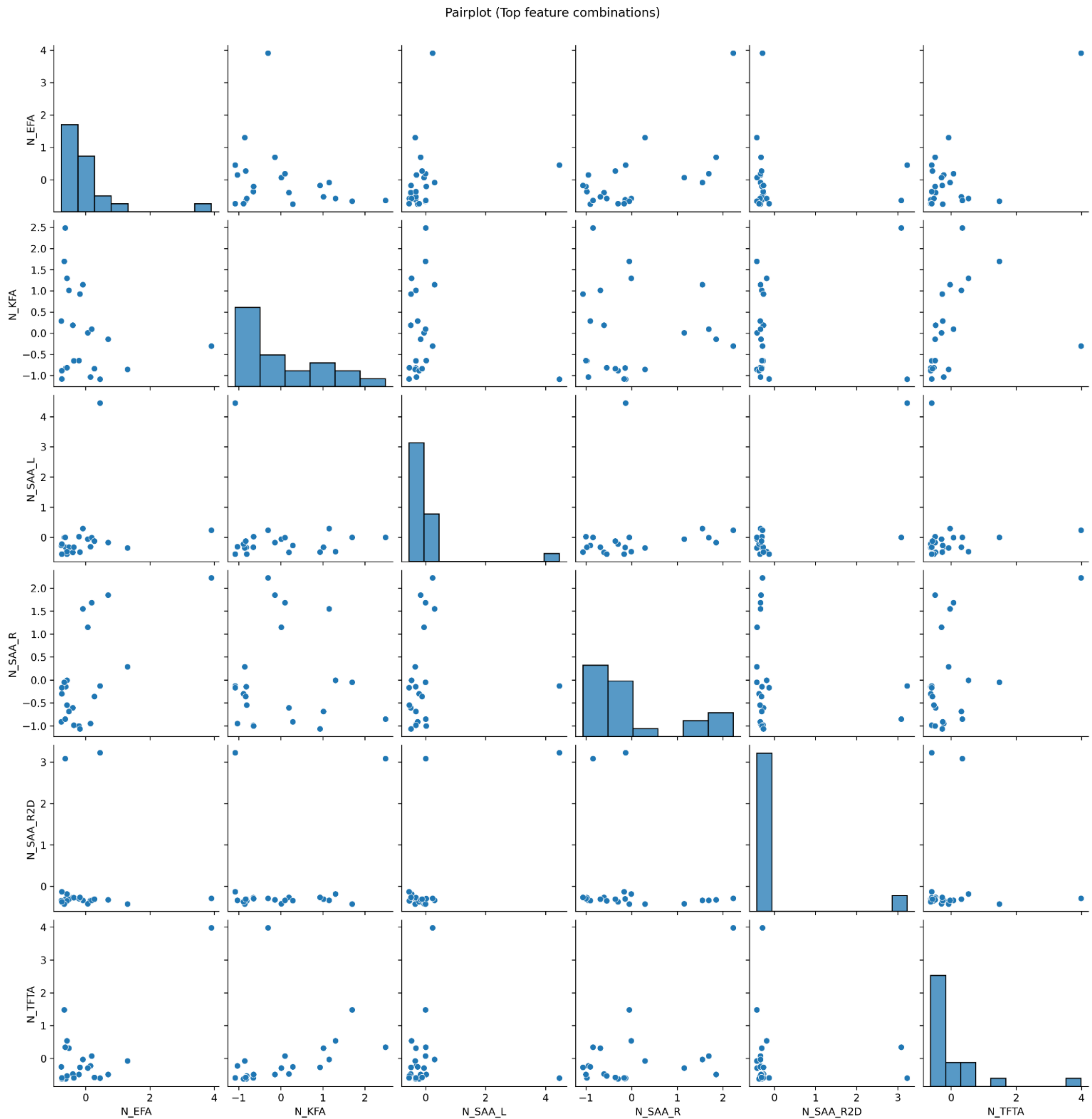

Figure 12. Pairwise relationships among selected features visualized using scatter plots with class labels.